

## Accepted Manuscript

Chitosan-based dressings loaded with neurotensin-an efficient strategy to improve early diabetic wound healing

Liane I.F. Moura, Ana M.A. Dias, Ermelindo C. Leal, Lina Carvalho, Hermínio C. de Sousa, Eugénia Carvalho

PII: S1742-7061(13)00504-7

DOI: <http://dx.doi.org/10.1016/j.actbio.2013.09.040>

Reference: ACTBIO 2932

To appear in: *Acta Biomaterialia*

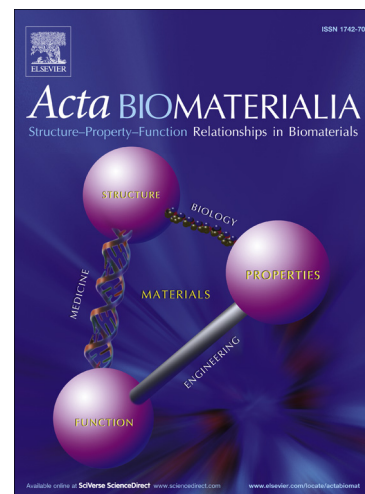
Received Date: 11 June 2013

Revised Date: 20 September 2013

Accepted Date: 30 September 2013

Please cite this article as: Moura, L.I.F., Dias, A.M.A., Leal, E.C., Carvalho, L., de Sousa, H.C., Carvalho, E., Chitosan-based dressings loaded with neurotensin-an efficient strategy to improve early diabetic wound healing, *Acta Biomaterialia* (2013), doi: <http://dx.doi.org/10.1016/j.actbio.2013.09.040>

This is a PDF file of an unedited manuscript that has been accepted for publication. As a service to our customers we are providing this early version of the manuscript. The manuscript will undergo copyediting, typesetting, and review of the resulting proof before it is published in its final form. Please note that during the production process errors may be discovered which could affect the content, and all legal disclaimers that apply to the journal pertain.



**Chitosan-based dressings loaded with neurotensin-an efficient strategy  
to improve early diabetic wound healing**

Liane I. F. Moura<sup>1,2</sup>, Ana M. A. Dias<sup>2</sup>, Ermelindo C. Leal<sup>1</sup>, Lina Carvalho<sup>3</sup>, Hermínio  
C. de Sousa<sup>2\*</sup>, Eugénia Carvalho<sup>1,4\*</sup>

<sup>1</sup>*Center of Neuroscience and Cell Biology, University of Coimbra, 3004-517 Coimbra, Portugal*

<sup>2</sup>*CIEPQPF, Chemical Engineering Department, FCTUC, University of Coimbra, Rua Sílvio  
Lima, Pólo II – Pinhal de Marrocos, 3030-790 Coimbra, Portugal*

<sup>3</sup>*Institute of Pathology, Faculty of Medicine, University of Coimbra, 3004-517 Coimbra,  
Portugal*

<sup>4</sup>*APDP, The Portuguese Diabetes Association, Rua do Salitre, n.º. 118-120, 1250-203 Lisboa,  
Portugal*

\*Corresponding authors:

Eugénia Carvalho  
Center for Neurosciences and Cell Biology,  
University of Coimbra,  
3004-517 Coimbra, Portugal  
Phone: +351 239 855 760  
Fax: +351 239 853 409  
E-mail address: [ecarvalh@cnc.uc.pt](mailto:ecarvalh@cnc.uc.pt)

Hermínio C. de Sousa  
CIEPQPF, Chemical Engineering Department, Faculty of Science and Technology,  
University of Coimbra,  
3030-790 Coimbra, Portugal  
Phone: +351 798 700  
Fax: +351 798 703  
E-mail address: [hsousa@eq.uc.pt](mailto:hsousa@eq.uc.pt)

**Abstract**

One important complication of *diabetes mellitus* is the chronic, non-healing diabetic foot ulcer (DFU). This study aims to develop and use dressings based on chitosan derivatives for the sustained delivery of the neurotensin (NT), a neuropeptide that act as an inflammatory modulator in wound healing. Three different derivatives, namely N-carboxymethyl chitosan (CMC), 5-methyl pyrrolidinone chitosan (MPC) and N-succinyl chitosan (SC), are presented as potential biomaterials for wound healing applications. Our results showed that MPC has the best fluid handling capacities and delivery profile being also non-toxic to Raw 264.7 and HaCaT cells. NT-loaded and non-loaded MPC dressings were applied into control/diabetic wounds to evaluate their *in vitro/in vivo* performances and the results show that the first induced a faster healing (50% wound area reduction) in the early phases of wound healing in diabetic mice. NT-loaded MPC foam also reduced inflammatory cytokines expression namely TNF- $\alpha$  ( $p<0.001$ ) and decreased the inflammatory infiltrate at day 3. At day 10, MMP-9 is reduced in diabetic skin ( $p<0.001$ ) increasing significantly fibroblasts migration and collagen (COL1A1, COL1A2 and COL3A1) expression and deposition. These results suggest that MPC-based dressings may work as an effective support for a NT sustained release to modulate DFU.

**Keywords:** Chitosan derivatives; wound dressings; diabetic foot ulcers; neurotensin; wound healing

**Abbreviations:**

79	Collagen type I, alpha 1 (COL1A1)
80	Collagen type I, alpha 2 (COL1A2)
81	Collagen type III, alpha 1 (COL3A1)
82	Diabetic foot ulcer (DFU)
83	Ditio-bis(nitrobenzoic acid) (DTNB)
84	Endothelial growth factor (EGF)
85	Extracellular Matrix (ECM)
86	Fetal bovine serum (FBS)
87	Glutathione (GSH)
88	Interleukin-1 $\beta$ (IL-1 $\beta$ )
89	Interleukin-6 (IL-6)
90	Interleukin-8 (KC)
91	Metalloproteinase 9 (MMP-9)
92	N-carboxymethylchitosan (CMC)
93	Neurotensin (NT)
94	Nitric oxide (NO)
95	N-succinyl chitosan (SC)
96	Phosphate buffer solution (PBS)
97	Platelet-derived growth factor (PDGF)
98	Polymorphonuclear leukocytes (PMN)
99	Scanning electron microscopy (SEM)
100	Streptozotocin (STZ)
101	Transforming growth factor $\beta$ 1 (TGF $\beta$ 1)
102	Transforming growth factor $\beta$ 3 (TGF $\beta$ 3)
103	Tumor Necrosis Factor - $\alpha$ (TNF- $\alpha$ )
104	Vascular endothelial growth factor (VEGF)

106

107

108

109

110

111

## 1. Introduction

*Diabetes mellitus* is one of the most prevalent chronic diseases worldwide. Impaired wound healing is a complication of diabetes that results in the failure to completely heal diabetic foot ulcers (DFUs) [1]. Complications of DFUs lead to frequent hospitalizations and in extreme cases, to amputations that result in elevated hospital costs and poor quality of life for patients [2]. DFU is a multifactorial complication that results particularly as a consequence of peripheral neuropathy, impaired vascular function, impaired angiogenesis and/or chronic inflammation [1, 3].

Recently, it became evident that peripheral nerves and cutaneous neurobiology contributes to wound healing [4]. Loss of peripheral sensory and autonomic nerves reduces the production of neuropeptides that are important for proper wound healing [3]. Neurotensin (NT) is a bioactive neuropeptide that is widely distributed in the brain and in several peripheral tissues [5, 6]. NT interacts with leukocytes, mast cells, dendritic cells and macrophages leading to cytokine release and chemotaxis that can modulate the immune response. In addition, NT affects microvascular tone, vessel permeability, vasodilation/vasoconstriction and new vessel formation which helps to improve angiogenesis during wound healing processes [3, 7, 8].

Some studies demonstrated that topical application of neuropeptides, such as substance P and neuropeptide Y can improve wound healing in diabetes [9, 10]. However, the major problem of topical administration of peptides is their short half-life and loss of bioactivity in the peptidase-rich wound environment [11]. An alternative strategy to overcome this problem is the use of biocompatible wound dressings for the sustained delivery of neuropeptides. These dressings should however also replicate skin characteristics in order to promote the proliferation and migration of fibroblasts and keratinocytes, as well as to enhance collagen synthesis, leading to proper healing with low scar formation [12, 13].

Wound dressings based on natural polymers have been extensively applied to simulate extracellular matrix (ECM) regeneration after injury [12, 13]. One of the most used natural-based polymer for wound healing applications is chitosan [12], which is a linear copolymer of D-glucosamine and N-acetyl-D-glucosamine [14]. Since it is derived from chitin, a polymer found in fungal cell walls and crustacean exoskeletons, it is a relatively inexpensive and abundant material [15]. In addition, it has proven to be biodegradable, biocompatible, non-antigenic, non-toxic, bioadhesive, anti-microbial,

145 bioactive and to have haemostatic capacity [15-17]. Furthermore, chitosan promotes  
 146 tissue granulation and accelerates wound healing through the recruitment of  
 147 inflammatory cells such as polymorphonuclear leukocytes (PMN) and macrophages to  
 148 the wound site [18].

149 To increase its poor solubility in water, chitosan functional groups can be chemically  
 150 modified to originate water soluble chitosan derivatives such as *N*-carboxymethyl  
 151 chitosan (CMC), 5-methyl pyrrolidinone chitosan (MPC) and *N*-succinyl chitosan (SC)  
 152 [19-21]. These chitosan derivatives are functional biomaterials that maintain the  
 153 antibacterial and non-cytotoxic properties of parent chitosan. In addition, they stimulate  
 154 extracellular lysozyme activity of skin fibroblasts [22, 23].

155 The aim of this study was to develop and apply wound dressings, prepared from the  
 156 chitosan derivatives referred above (CMC, MPC, SC), for a prolonged and efficient NT  
 157 delivery into diabetic and non-diabetic wounds, and also confer wound protection and  
 158 comfort. The progression of skin wound healing in diabetic and non-diabetic mice was  
 159 also evaluated by the analysis of the inflammatory and angiogenic effects of NT when  
 160 applied in skin wounds alone or loaded into MPC-based dressings.

161

## 162 **2. Materials and methods**

### 163 **2.1 Materials**

164 Chitosan (medium molecular weight, degree of acetylation of 90% confirmed by <sup>1</sup>H-  
 165 NMR), glyoxylic acid monohydrate (98%), sodium hydroxide, sodium borohydride  
 166 (99.5%), levulinic acid (98%), succinic anhydride (97%), reduced GSH, DTNB, dialysis  
 167 membranes (Spectra/Por (6)) with a MWCO of 8000 Da and methanol p.a., were  
 168 obtained from Sigma-Aldrich (USA). Acetic acid was obtained from Panreac (Spain),  
 169 and ethanol was purchased from Riedel-de-Haen (Germany). Ketamine (Clorketam  
 170 1000) was obtained from Vétoquinol (Portugal) and xylazine (Rompun) from Bayer  
 171 HealthCare (Germany). NT was purchased from Bachem (Switzerland). The antibodies  
 172 against TNF- $\alpha$  and MMP-9 were purchased from Cell Signaling Technology (USA) and  
 173 the antibodies against VEGF and actin were purchased from the Millipore Corporation  
 174 (USA).

175

176

177

## 178 2.2 Synthesis of chitosan derivatives CMC, MPC, SC

179 Chitosan (2 g) reacted with glyoxylic acid (1,16 g), levulinic acid (5ml) or succinic  
180 anhydride (3 g) to synthesize CMC, MPC and SC respectively [24, 25], following by  
181 precipitation with ethanol and dialysis to remove unreacted reagents. Foams of CMC,  
182 MPC and SC were prepared by freeze-drying adding 1.5 ml of each solution in 12 multi  
183 well plates. The average thickness of the obtained materials was  $250 \pm 15$   $\mu\text{m}$ . All  
184 samples were stored at  $-20$   $^{\circ}\text{C}$ , away from light and humidity before usage. The degree  
185 of substitution of each of the derivatives was calculated by  $^1\text{H-NMR}$  using a Bruker  
186 Avance III 400 MHz spectrometer, with a 5-mm TIX triple resonance detection probe  
187 using  $\text{D}_2\text{O}$  acidified with acetic acid (10  $\mu\text{l}$  of acetic acid in 600  $\mu\text{l}$  of  $\text{D}_2\text{O}$ ).

## 189 2.3 Scanning electron microscopy (SEM)

190 SEM micrographs were obtained at 5 kV (Jeol, model JSM-5310, Japan). Samples were  
191 coated with gold (approximately 300  $\text{\AA}$ ) in an argon atmosphere.

## 193 2.4 Water vapor and water sorption capacities

194 Samples of CMC, MPC and SC, with 22 mm of diameter, were dried at  $37$   $^{\circ}\text{C}$  for 72 h  
195 until constant weight was achieved. Both water vapor and water sorption capacities  
196 were measured gravimetrically. In the first case, dried foams were exposed to a 95%  
197 relative humidity atmosphere, in a desiccator containing a saturated solution of  
198 potassium sulfate at  $32$   $^{\circ}\text{C}$  accordingly to Dias et al, 2013 [26]. In the second case,  
199 samples were immersed into phosphate buffer (pH 7) at  $37$   $^{\circ}\text{C}$  and weighted after  
200 removing the surface phosphate buffer using filter paper.

201 Samples were weighted at fixed time intervals until they reach equilibrium. The water  
202 vapor and water sorption capacities were calculated as the ratio between sample weight  
203 at time  $t$  and sample initial dry weight. All the samples were measured in duplicate.

## 205 2.5 *In vitro* release kinetics

206 Kinetic release profiles of GSH were performed spectrophotometrically (Jasco, model  
207 630, Japan) at 412nm. Known amounts of a GSH solution (5 mM) were loaded into  
208 previously weighted samples of each polymer. The GSH solution has been previously  
209 placed in an ultrasonic bath to avoid oxidation. After drying, samples were immersed in  
210 phosphate buffer at pH 6, 7 or 8 at  $32$   $^{\circ}\text{C}$ , under orbital stirring (100 rpm) during 8 h.

211 The quantification of released GSH was based on the Ellman's Test. This test is based  
212 on the addition of 5,5'-dithio-*bis*-(2-nitrobenzoic acid) (DTNB), a yellow water-soluble  
213 compound, that reacts with free sulfhydryl groups in peptide solution. At pre-  
214 determined time periods, an aliquot (100  $\mu$ l) of the released solution was removed and  
215 analyzed with a mixture of 1800  $\mu$ L of phosphate buffer and 100  $\mu$ l of DNTB stock  
216 solution (20 mM). Fresh 100  $\mu$ L of phosphate buffer was added each time point to the  
217 medium. Each sample was analyzed in duplicate.

218

## 219 **2.6 Cell culture**

220 Mouse leukaemic monocyte macrophages (Raw 264.7) and human keratinocyte  
221 (HaCaT) cells were cultured in DMEM medium, pH 7.4, supplemented with 10 % heat  
222 inactivated fetal bovine serum (FBS), 3.02 g/l sodium bicarbonate, 30 mM glucose, 100  
223 U/ml penicillin, 100  $\mu$ g/ml streptomycin, at 37 °C in a humidified incubator containing  
224 5% CO<sub>2</sub>. Sub-culturing was performed according to ATCC recommendations. Raw  
225 264.7 and HaCaT cell lines were purchased by ATCC (number TIB-71) and CLS  
226 (number 300493), respectively.

227

## 228 **2.7 MTT assay**

229 Raw 264.7 ( $8 \times 10^4$  cells/well) and HaCaT ( $4 \times 10^4$  cells/well) cells were plated  
230 individually in 12-well plates with 430  $\mu$ L of DMEM, above the previously sterilized  
231 biomaterials (UV light for at least 30 minutes). After 24 and 48 h of incubation, 43  $\mu$ l  
232 of 3-(4,5-dimethylthiazol-2-yl)-2,5-diphenyltetrazolium bromide (MTT) solution  
233 (5mg/ml) was added to each well. The plates were further incubated at 37 °C for 1 h, in  
234 a humidified incubator containing 5% CO<sub>2</sub>. After this period, 300  $\mu$ l of acidic  
235 isopropanol (0.04 N HCl in isopropanol) was added. Quantification was performed  
236 using an ELISA automatic microplate reader (SLT, Austria) at 570 nm, with a reference  
237 wavelength of 620 nm. Each sample was analyzed in duplicate.

238

## 239 **2.8 NO production – Griess Method**

240 Raw 264.7 ( $8 \times 10^4$  cells/well) cells were plated in 12-well plates with 430  $\mu$ L of DMEM,  
241 above the previously sterilized biomaterials (UV light for at least 30 minutes). After 24  
242 and 48 h after incubation, 170  $\mu$ l of medium supernatant was mixed with an equal  
243 volume of Griess reagent (1% sulfanilamide, 0.1% N-1-naphthelenediamine



244 dihydrochloride in 2.5% phosphoric acid). After 30 minutes of incubation in the dark,  
 245 the absorbance was measured at 550 nm in a microplate reader (SLT, Austria). Nitrite  
 246 concentration was calculated from a previously obtained nitrite standard curve.

247

## 248 **2.9 *In vivo* wound closure**

249 We used male C57BL/6 mice (Charles River Corporation Inc, Barcelona, Spain)  
 250 weighing 25-30 g. The animals were maintained at normal room temperature (22-24 °C)  
 251 on a 12 h light/dark cycle, with free access to commercial pellet diet and water. After  
 252 the wound procedure, the animals were kept in individual cages. All experiments were  
 253 conducted according to the National and European Communities Council directives on  
 254 animal care.

255 Diabetes was induced by a single intraperitoneal injection of streptozotocin (STZ, 150  
 256 mg/kg) in citrate buffer pH 4.5. Four days after diabetes induction, blood glucose levels  
 257 were checked by Accu-Chek Aviva glucometer (Roche Diagnostics GmbH, Germany).  
 258 The animals with blood glucose levels higher than 300 mg/dl were considered diabetic.  
 259 Mice were anesthetized by intraperitoneal injection of xylazine (13 mg/kg) and  
 260 ketamine (66.7 mg/kg). The dorsal hair of control and diabetic mice was shaved and  
 261 two 6 mm diameter full-thickness wounds were created with a biopsy punch.

262 C57BL/6 mice were randomly divided into six groups of treatment for control (non-  
 263 diabetic) and diabetic mice – three groups for day 3 (d3) (I, II, III) and three similar  
 264 groups for day 10 (d10) (IV, V, VI): groups I and IV were treated with MPC dressings  
 265 alone (6-12 animals), groups II and V with topical application of 50 µg/ml NT (7  
 266 animals) and groups III and VI with 50 µg/ml NT-loaded MPC dressings (7-9 animals).

267 For each animal one of the wounds worked as control (PBS application only) and the  
 268 other received treatment. The dried MPC foams were applied over the wounds and  
 269 wetted with 5 µl of PBS or NT solution (50 µg/ml) to originate hydrogels with improved  
 270 adherence and mucoadhesive capacities. By visual inspection it was possible to observe  
 271 that the dressings persist into the wound approximately until day 6-7. The progress of  
 272 wound healing was evaluated periodically by acetate tracing till day 10. Topical  
 273 application of PBS or NT (alone or loaded into the prepared MPC dressing) was  
 274 performed daily. At day 3 or day 10, C57BL/6 mice were sacrificed and around 2 mm  
 275 of tissue and skin surrounding the wound were harvested. These time points were

276 chosen to evaluate the inflammatory (day 3) and the proliferating/remodeling (d10)  
277 phases of wound healing.

278

## 279 **2.10 Real time RT-PCR**

280 Total RNA was isolated from skin with the RNeasy Mini Kit according to the  
281 manufacturer's instructions (Qiagen, USA). First strand cDNA was synthesized using  
282 High Capacity cDNA Reverse Transcription. Then, real-time RT-PCR was performed  
283 in a BioRad MyCycler iQ5. Primer sequences are given upon request. Gene expression  
284 changes were analyzed using iQ5Optical system software v2. The results were  
285 normalized using a housekeeping gene, TATA box binding protein (TBP), which was  
286 previously validated in our lab. Quantitative RT-PCR results were analyzed through  
287 delta CT calculations.

288

## 289 **2.11 Western Blotting**

290 Skin tissue lysate was homogenized in RIPA buffer (50mM Tris HCl pH8, 150 mM  
291 NaCl, 1% NP-40, 0.5% Sodium Deoxycholate, 0.1% SDS, 2 mM EDTA, proteases  
292 inhibitor cocktail, phosphatase inhibitor cocktail and 1 mM DTT). Protein concentration  
293 was determined using the BSA method and the skin lysates were denatured at 95 °C, for  
294 5 min, in sample buffer. 40 µg of total protein were resolved on 12% SDS-PAGE and  
295 transferred to PVDF membranes. The membranes were blocked with 5% fat-free dry  
296 milk in Tris-buffered saline containing 0.1% (v/v) Tween 20 (TBS-T), for 1 h, at room  
297 temperature. After blocking, membranes were incubated with the primary antibodies  
298 against the TNF- $\alpha$  (1:500), VEGF (1:1000), MMP-9 (1:500), overnight at 4 °C. After  
299 incubation, membranes were washed and incubated for 1 h at room temperature, with  
300 anti-rabbit antibody (1:5000), or anti-mouse antibody (1:5000). The membranes were  
301 exposed to the ECF reagent followed by scanning on the VersaDoc (Bio-Rad  
302 Laboratories, Portugal). For normalization, the membranes were re-probed with an anti-  
303 actin antibody (1:10000). The generated signals were analyzed using the Image-Quant  
304 TL software.

305

## 306 **2.12 Hydroxyproline content**

307 This analysis was performed using a Hydroxyproline Assay Kit (Sigma Aldrich, USA).  
308 Briefly, 10 mg of skin tissue were homogenized in 100 µl of water and hydrolyzed with

HCl 12 M at 120 °C for 3 h. 25 µl of the supernatant were transferred to 96- well plate and evaporated in the incubator at 60 °C till total dryness. After, 100 µL of the Chloramine T/Oxidation Buffer and 100 µL of the Diluted DMAB Reagent were added to each sample and incubated for 90 minutes at 60 °C. Quantification was performed using an ELISA automatic microplate reader (SLT, Austria) at 560 nm.

### 2.13 Histopathological analysis

For histological preparation, the skin was fixed in 10% neutral buffered formalin and then embedded in paraffin. Skin tissues were sectioned in 3 µm thickness slices for histopathological examination by hematoxylin/eosin (H&E) and for collagen formation by Masson's Trichrome staining, using standard procedures. The stained sections were observed with a microscope Nikon H600L with Digital Camera DXM 1200F (Nikon, Germany). Analysis of stained skin sections was performed by an experienced pathologist.

### 2.14 Statistical analysis

Results are expressed as mean  $\pm$  SEM (Structural Equation Modeling). Statistical analysis was performed using one-way ANOVA followed by Tukey's multiple comparison tests or through the unpaired or paired t test by GraphPad Prism (GraphPad Software, Inc., San Diego, CA, USA) and p values lower than 0.05 were considered statistically significant.

## 3. Results

### 3.1 Degree of substitution and morphology of CMC, MPC and SC

The degree of substitution (amount of native chitosan amino groups substituted) of each chitosan derivative was confirmed by <sup>1</sup>H-NMR and it was equal to 25.5%, 24% and 28.5% for CMC, MPC and SC, respectively (Figure S1 supplementary data). The schematic representation of each derivative is shown in Figure 1A.

The different morphologies obtained for each of the prepared chitosan derivative foams are shown in Figure 1B. CMC presents a honeycomb-like porous structure, with larger pores than MPC and SC, which presented an interlaced fiber-like pattern. The fiber-like structure of SC seems to be thinner than the one observed for MPC.

### 3.2 Water vapor and water swelling properties

Figure 2A shows the water vapor sorption behavior of CMC, MPC and SC foams in controlled humidity (95%) and temperature conditions (32 °C). Data show that the hydrophilicity of the materials changes in the sequence SC > MPC > CMC. All the samples achieved equilibrium after approximately 8 hours and at this point, SC adsorbed 35% of its weight in water vapor while MPC and CMC adsorbed 24% and 14%, respectively.

In terms of water swelling capacity, Figure 2B shows that SC presents the fastest swelling rate, reaching its maximum (2438%) after 5 h and it starts to dissolve after this period. On the other hand, CMC presented the lowest swelling capacity (163%) while MPC has an intermediate water swelling profile. Both MPC and SC foams reach water swelling equilibrium after approximately 6 h and both maintain their structure (macroscopically, at naked eye) until day 15, at the tested experimental conditions.

### 3.3 *In vitro* release kinetics

Glutathione (GSH) was used as a model peptide test molecule for *in vitro* release kinetics studies. The release of GSH from CMC, MPC and SC foams was followed for a period of 8 h at 3 different pHs (6, 7 and 8) which is the pH range that can be observed during the wound healing process. The release profiles measured for each chitosan derivative at pH 7 are presented in Figure 3. Data measured at pHs 6 and 8 are presented as supplementary data (Figure S2) due to the similarities observed among the different pHs studied in this work. The release profiles show that equilibrium is attained between 5 and 8 h for all the samples and that the amount of GSH released from SC is significantly higher than for CMC and MPC (~9 and 4 times higher, respectively). When comparing the amount of GSH released after 8 h with the total GSH loaded amount, the results show that ~50% was released from CMC and MPC while almost 100% was released from SC. Obtained results also show that the amount of GSH released from the chitosan derivatives is not significantly affected in the pH range studied and considering the experimental error, being average equal to  $(32.33 \pm 0.72)$ ,  $(67.65 \pm 6.77)$  and  $(287.18 \pm 14.92)$  GSH released (%) /  $m_{\text{polymer}}$  (g) for CMC, MPC and SC, respectively.

### 3.4 *In vitro* biocompatibility of CMC and MPC

There was no significant difference in the viability of the Raw and HaCaT cells exposed to CMC and MPC foams during 24, 48 and 72 h, when compared to control, as shown in Figure 4 (A and B, respectively). NO is produced by macrophages in response to an inflammatory stimuli. The production of nitrites, final stable breakdown product of NO, measured after exposure of the cells to the chitosan derivatives (Figure 4C) was also not significantly affected, however, a slight increase in the nitrites produced after 72 h was observed, which may be due to the stress to which cells are subjected after this exposure period.

### 3.5 Wound healing experiments – *in vivo*

Figure 5 shows the effect of the different topical treatments studied in this work: NT alone, MPC foam alone and NT-loaded MPC foam both in control (A) and diabetic (B) mice. PBS was applied as control. All treatments were shown to reduce significantly the wound area, as compared to PBS treated wounds, in both control and diabetic mice. In Figure 5 A, NT alone reduced significantly the wound size at day 3 post wounding, by 22% ( $p<0.05$ ), compared to the PBS treated wounds, in control mice. In diabetic mice, the wound size of the NT treated wounds is also significantly reduced at day 3, and at day 5 by 29% ( $p<0.01$ ) and 34% ( $p<0.01$ ), respectively. A different healing profile is observed for the non-loaded and NT-loaded MPC treated wounds either in control and diabetic mice. A significant decrease in the wound area is evident at day 1 post wounding in non-loaded MPC by 48% ( $p<0.001$ ) and in NT-loaded MPC, by 43% ( $p<0.001$ ), when compared with PBS-treated wounds (Figure 5A). In diabetic animals, the profile of wound closure was similar, however the NT-loaded MPC treatment was significantly more effective than MPC alone, with a wound reduction of 50% ( $p<0.001$ ) instead of 35% ( $p<0.001$ ) of closure for the non-loaded dressing (Figure 5B).

### 3.6 Cytokine, MMP-9, collagen types and growth factors expression at the wound site

In order to address the pattern of cytokine gene expression in untreated or treated wounds at 0, 3 and 10 days post-wounding, the gene expression for inflammatory cytokines (TNF- $\alpha$ , IL-6, KC, IL-1 $\beta$ ) and several types of collagen genes (COL1A1, COL1A2, COL3A1) were measured and the results are presented in Figure 6 A-N. Other important factors such as MMP-9, growth factors (EGF, VEGF, PDGF), TGF $\beta$ 1,

408 TGF $\beta$ 3 were also evaluated and its expressions are presented in Figure S3  
409 Supplementary data.

410 In unwounded skin (day 0, baseline), all the measured inflammatory cytokines were  
411 significantly increased in the skin of diabetic animals compared with the healthy  
412 controls (Figure 6 A-G). On the other hand, all types of collagens analyzed are  
413 significantly reduced ( $p<0.001$ ) (Figure 6 I-N, respectively).

414 We observed a significant increase, at day 3 post-wounding, in the inflammatory  
415 stimulus, as one might expect, when compared to day 0 in controls. However, the same  
416 effect is not observed in diabetic mice.

417 Furthermore, at day 3, in control mice, the MPC treatment alone reduced significantly  
418 the expression of TNF- $\alpha$  ( $p<0.05$ ), IL-6 ( $p<0.05$ ) and IL-1 $\beta$  ( $p<0.05$ ) while the NT  
419 alone decreased the expression of TNF- $\alpha$  ( $p<0.05$ ) and IL-1 $\beta$  ( $p<0.05$ ) (Figure 6 A, C  
420 and G, respectively). In addition, the NT-loaded MPC treatment reduced the TNF- $\alpha$   
421 expression ( $p<0.05$ ), however the IL-6 and KC expression significantly increased in the  
422 controls ( $p<0.05$ ). In diabetic mice, the TNF- $\alpha$  expression was significantly higher for  
423 all treatments ( $p<0.05$ ) but the IL-1 $\beta$  expression is reduced upon the NT-loaded MPC  
424 treatment ( $p<0.05$ ) compared with PBS alone.

425 Moreover, at day 3, NT alone reduced the EGF expression in diabetic mice ( $p<0.05$ )  
426 and increased the VEGF expression ( $p<0.05$ ) in the control (Figure S3 C and E). In  
427 addition, while NT and NT-loaded MPC foam significantly induced TGF $\beta$ 3 expression  
428 ( $p<0.001$ ), in controls, no differences were observed in diabetic skin (Figure S3 K).  
429 Collagen genes were more expressed in control skin and NT treatment significantly  
430 increased COL1A1, COL1A2 and COL3A1 expression in diabetic skin (Figure 6 I, K  
431 and M, respectively).

432 At day 10, the expression of all the inflammatory cytokines was diminished to baseline  
433 levels in the controls, with the exception of TNF- $\alpha$  that increase ( $p<0.05$ ) with NT and  
434 the NT-loaded MPC application, compared to PBS treated wounds. In diabetic mice, all  
435 the treatments reduced the expression of TNF- $\alpha$ , IL-6 and KC ( $p<0.05$  in all cases)  
436 (Figure 6 B, D and F, respectively). The non-loaded and the NT-loaded MPC treatments  
437 caused a decrease in the MMP-9 expression in both control and diabetic mice ( $p<0.05$ )  
438 (Figure S3 B). In addition, the NT-loaded MPC treatment reduced EGF in diabetic  
439 mouse skin ( $p<0.05$ ) (Figure S3 D).

NT and NT-loaded MPC foam significantly induced TGF $\beta$ 1 and TGF $\beta$ 3 expression ( $p<0.001$ ) in controls at day 10 but no differences were observed in diabetic skin. In diabetic skin, only NT treatment reduced significantly TGF $\beta$ 3 ( $p<0.05$ ) (Figure S3 J, L). In addition, NT and NT-loaded MPC foam highly stimulated an increase in COL1A1 and COL1A2 ( $p<0.001$ ) in control mice while in diabetic mice only NT-loaded MPC significantly induced expression of all collagen genes (Figure 6 J, L,N).

### 3.7 Protein expression in the wound site

To evaluate protein expression levels at the wound site, Western Blot analysis of skin tissue was performed (Figure 7). At day 0, only MMP-9 is significantly increased ( $p<0.001$ ) in diabetic mice when compared to controls. At day 3, NT treatment induced a reduction of MMP-9 protein levels in control mice. Moreover, in diabetic wounds, MPC treatment increased TNF- $\alpha$  level. In contrast, NT and NT-loaded MPC foam significantly reduced MMP-9 ( $p<0.05$ ) and TNF- $\alpha$  ( $p<0.001$ ) protein levels, respectively.

At day 10, MPC, NT or NT-loaded MPC treatments significantly reduced MMP-9 protein expression comparing with PBS treatment, either in control or diabetic skin. In addition, TNF- $\alpha$  protein expression was not detected in all treatments at day 10, by Western Blot.

### 3.8 Hydroxyproline content in the wound site

To evaluate collagen deposition in mouse skin, hydroxyproline levels were measured in unwounded and wounded (treated and non-treated) skin (Figure 8). In unwounded skin, hydroxyproline levels were significantly decreased ( $p<0.01$ ) in diabetic mice comparing with control skin. At day 3 post-wounding, NT significantly increased ( $p<0.05$ ) hydroxyproline content in diabetic skin, while at day 10, this effect was observed with NT-loaded MPC in control and diabetic skin ( $p<0.05$ ,  $p<0.01$ ), respectively.

### 3.9 Histopathological analysis of the wound

For the histopathological analysis of control and diabetic skin tissue we used the H&E and Masson's Trichrome staining (Figures 9A and B, respectively). In unwounded skin the increase in the epidermis skin thickness was evident in diabetic mice when compared with control. At day 3 post wounding, all the treatments stimulated an



473 increase in the epidermis thickness which was more significant for the non-loaded and  
 474 NT-loaded MPC treatments in diabetic skin (Table 1). At day 10, the epidermis  
 475 thickness profile was similar with a stronger effect in diabetic skin (Figure 9A – 3),  
 476 (Table 2). A specific re-epithelialization profile was observed: in control mice, re-  
 477 epithelialization occurred from bottom to top with basal cells in the epidermis covering  
 478 the scar. In diabetic mice, the re-epithelialization occurred over the granulation  
 479 inflammatory tissue while this was suffering repair, without correlation with the applied  
 480 treatments, in both groups (Table 2 and 3).

481 At day 3, neither MPC, NT alone or NT-loaded MPC treatments affected the number of  
 482 polymorphonuclear leukocytes (PMN) and lymphocytes in control skin, however in  
 483 diabetic skin, these inflammatory cells were less recruited to the wound site compared  
 484 with the PBS treatment. In addition, there is higher production of fibrin in diabetic skin  
 485 while no plasma cells were observed in either control or diabetic skin (Table 3). At day  
 486 10, there was no significant recruitment of PMN and lymphocytes observed in control  
 487 skin, while in diabetic wounds treated with either MPC, NT alone or NT-loaded MPC,  
 488 PMN cells, lymphocytes and plasma cells were present in higher numbers when  
 489 compared with PBS treatment. It is important to note that inflammatory cells persisted  
 490 at day 10 especially in the diabetic wounded skin. No fibrin was observed either in  
 491 control or diabetic skin (Table 4). Fibroblasts, which are important for tissue repair,  
 492 were increased in diabetic when compared to control wounded skin, at day 3. Moreover,  
 493 collagen matrix production appeared to be more evident in diabetic skin, particularly  
 494 after the NT or the NT-loaded MPC foam treatment. However, the scar was more  
 495 pronounced in these treatments (Table 3). Furthermore, at day 10, NT-loaded MPC  
 496 foam induced the migration of fibroblasts and the production of the collagen matrix.  
 497 However, the scar obtained after this treatment was more pronounced (Table 4). A  
 498 summary of cytokine expression and corresponding cell type production, in wounded  
 499 control and diabetic skin, at either day 3 or 10 post-wounding, is represented on table 5.

500

#### 501 **4. Discussion**

502 One of the main objectives of this work was to evaluate the capacity of chitosan-based  
 503 wound dressings to work as biocompatible and biodegradable supports for the sustained  
 504 delivery of neurotensin (NT), a neuropeptide that has shown to improve wound healing  
 505 [27, 28].



Three different water soluble chitosan derivatives (CMC, MPC and SC) were synthesized and tested for their water swelling capacities and peptide release profiles in order to infer which of the derivatives would present the best performance (controlled swelling and NT delivery over time) *in vivo*. At this stage, GSH was used as a model peptide. Although GSH presents lower molecular weight than NT, it has similar functional groups that will permit the simulation of the physical and chemical interactions that may be established between the molecule and the material used as the dressing.

The obtained results showed that the SC foam has the highest water vapor and water swelling capacity probably due to the high number of thin fibers that constitute its matrix, increasing the contact area between the material and the water molecules. The higher affinity of SC for water (higher hydrophilicity) justifies its faster dissolution in PBS. These results are also in agreement with the  $^1\text{H-NMR}$  data that showed a higher degree of substitution for SC. This was expected since chitosan substitutions performed in this work aimed to improve the solubility of chitosan in aqueous media. According to the water swelling results, MPC presented an intermediate swelling profile, despite the apparent larger porosity of the CMC derivative observed by SEM analysis.

Medicated wound dressings have been largely used to deliver healing enhancers and therapeutic substances, such as growth factors or stem cells to stimulate wound healing [29, 30]. Their use allows the protection of the wound against external aggression and avoids the rapid biodegradation of the bioactive healing enhancers that may occur in the enzyme rich wound environment. In this work, the capacity of each dressing to sustain the release of a peptide at different pH conditions was addressed. The measured release kinetics performed was not significantly affected within the pH ranges studied and SC is the material that presented the faster release of GSH, followed by MPC and CMC. The release profiles are in accordance with the water swelling profiles observed for the different chitosan derivatives, indicating that the GSH release is mainly controlled by the water swelling capacity of the material and therefore GSH is released mainly through a diffusion mechanism. The higher swelling capacity of SC leads to a higher amount of water inside the polymer structure, better dissolving GSH, enhancing its release into the surrounding medium. According to these results (water swelling and GSH release data), and considering that sustained profiles were envisaged for *in vivo* applications, the use of SC based material was discarded at this stage.

539 The biocompatibility of CMC and MPC foams was tested *in vitro*, in Raw 264.7 and  
 540 HaCaT cell lines and the results showed that both materials were non-toxic against these  
 541 cell lines, up to 48 h. For the 72 h test period, a slight decrease (not statistically  
 542 significant) in the viability of the cells was observed probably due to foam dissolution  
 543 or cell stress in the media conditions. Similar results were observed in L929 cells  
 544 (fibroblast cell line) by Huang and colleagues [31]. The production of nitrites by  
 545 macrophages Raw 264.7 was also quantified since it is known that these cells produce  
 546 NO when stimulated by inflammatory stimulus. The results presented show that CMC  
 547 and MPC do not increase nitrite levels *in vitro* suggesting that these compounds do not  
 548 induce an inflammatory response which is in accordance with data previously reported  
 549 in the literature [32]. The *in vitro* results indicate that both CMC and MPC could be  
 550 used for wound dressing applications. However, in this work, *in vivo* application and  
 551 characterization was performed only for MPC, which was the material that presented an  
 552 intermediate GSH release profile compared to either CMC or SC.

553 Several studies suggested that chitosan and derivatives accelerate wound healing [33,  
 554 34]. For instance, MPC freeze-dried foams were shown to jellyfy in contact with  
 555 biological fluids, being progressively absorbed via enzymatic hydrolysis, promoting  
 556 regeneration of connective tissues [35]. However, no further studies were found in the  
 557 literature reporting the effect of MPC alone or in combination with NT in diabetic  
 558 wound healing.

559 *Diabetes mellitus* cause important complications, namely at skin level. The healing  
 560 process involves several overlapping phases: homeostasis/coagulation, inflammation,  
 561 proliferation (granulation tissue formation), re-epithelialization and remodeling [36].  
 562 All these processes require the interaction of skin cells, cytokines and growth factors  
 563 released from inflammatory cells, fibroblasts, keratinocytes and epithelial cells [2].

564 Due to the fact that mouse skin is elastic and has lack of a strong adherence to the  
 565 underlying structures, wound contraction is usually more rapid than epithelialization  
 566 which causes a decrease in the overall healing time of mice wounds [37]. Wound  
 567 closure results show that NT induced a faster closure in diabetic mice, even when  
 568 applied directly over the wound and compared with control mice. This was expected  
 569 since it has been reported that topical application of neuropeptides, such as Substance P,  
 570 stimulate diabetic wound healing [9]. In addition, previous studies in our group  
 571 observed that NT modulates inflammatory responses in a skin dendritic cell line [28].

572 Treatments with non-loaded and NT-loaded MPC foams induced a significant reduction  
 573 of the wound area, especially in the first 3 days post-wounding and in both control and  
 574 diabetic mice. Moreover, NT-loaded MPC presented a faster healing profile in diabetic  
 575 skin wounds. These results suggest a synergistic behavior between the bioactivity of NT  
 576 alone and the intrinsic healing properties of MPC. Moreover and as intended, a  
 577 sustained release of NT may also occur which guarantees controlled NT levels during  
 578 the healing process. The adhesive properties of chitosan and its derivatives could  
 579 explain this enhanced healing profile [38]. In addition, wound contraction is necessary  
 580 for the healing process, probably due to the enhanced proliferation of fibroblasts due to  
 581 arising contractile myofibroblasts [39]. Wound contraction is a biologically important  
 582 process in wound healing, especially in the healing of chronic wounds such as DFU,  
 583 although excessive contraction may lead to scar formation [40]. All treatments lead to  
 584 healing however, larger scars were developed over diabetic wounds that were treated  
 585 with MPC foams, most probably due to the fast initial wound contraction verified in this  
 586 case.

587 In unwounded diabetic skin, an overexpression of inflammatory cytokines, growth  
 588 factors and MMP-9 was observed, which is in agreement with the literature [41]. These  
 589 results suggest a chronic pro-inflammatory state in diabetic skin that can compromise  
 590 the wound healing. On the other hand, the gene expression of the different types of  
 591 collagen is down regulated in the diabetic skin suggesting a decreased capacity of the  
 592 diabetic skin to produce the appropriate matrix essential for wound healing and skin  
 593 repair. As decreased expression of COL1A1, COL1A2 and COL3A1 is verified, less  
 594 collagen is deposited as observed by the hydroxyproline assay [42].

595 In chronic diabetes, the healing process becomes stalled in one or more of the healing  
 596 phases originating chronic non-healing wounds. One important phase that can become  
 597 stalled in diabetes is the inflammatory phase [1]. TNF- $\alpha$ , IL-6, KC and IL-1 $\beta$  are  
 598 inflammatory cytokines involved in the recruitment of cells, such as neutrophils and  
 599 macrophages to the wound site, to stimulate the immune response. In the skin, TNF- $\alpha$   
 600 produced by inflammatory cells and fibroblasts stimulates adhesion molecules and  
 601 chemokines leading to attachment of inflammatory cells to vessels, rolling, migration,  
 602 and eventually chemotaxis into the skin [43]. Moreover, IL-6 and IL-1 $\beta$ , produced by  
 603 macrophages, fibroblasts, keratinocytes and epithelial cells are also important players in  
 604 the early phase of inflammation and in the wound healing process [44]. In control mice,

the reduction of TNF- $\alpha$  and IL-1 $\beta$  expression with all treatments, at day 3, suggests a decrease in the inflammatory condition which facilitates healing. In diabetic mice treated with MPC, NT or NT-loaded MPC, less infiltrated inflammatory cells was observed at day 3 comparing with control mice, while TNF- $\alpha$  expression is significantly higher, especially for the MPC alone. Moreover, IL-6 and KC expression is significantly reduced. These results may suggest that high expression of TNF- $\alpha$  is produced not only by inflammatory cells present at the wound site, but also by other cells present at day 3, which can stimulate contraction of the wound and consequently have a beneficial effect in the early stages of wound healing. This may further indicate that in diabetic mice, treated with NT or/and MPC, the granulation tissue fills the wound bed potentiated by the proliferation of skin fibroblasts, in the early phase of wound healing.

Similar results were observed when using MPC alone as treatment. However, NT-loaded MPC treatment induced a decrease in the TNF- $\alpha$  protein content suggesting that the combination of NT with the MPC foam has an effective anti-inflammatory role in wound healing.

At day 10, the inflammatory status persisted in diabetic mice while in controls it is resolved, as expected [4]. On the other hand, all treatments lead to a reduction in the inflammatory cytokines expression supported by the loose conjunctive tissue observed from the beginning, undergoing different status of collagen deposition in diabetic and control mice. At this time point, fibroblasts have an important role in collagen synthesis and scar formation [45, 46]. During the re-epithelialization phase, the initial ECM is gradually replaced by a collagenous matrix with the formation of new blood vessels [47]. The expression of angiogenic factors, VEGF and PDGF, did not change with treatments in diabetic mice possibly showing that these treatments do not stimulate the production of growth factors to improve wound healing.

Our results show that the production of the collagen matrix was higher for MPC and NT-loaded MPC treated diabetic skin, which is correlated with increased scar formation. Obara and colleagues [29] also observed that application of a chitosan hydrogel in diabetic wounds increased scar formation. Moreover, MMP-9 expression in diabetic skin wound was increased at day 3. Most importantly, at day 10, it is observed a decrease of MMP-9 in NT-loaded MPC treated diabetic wounds, while no significant effect is observed in control wounds. Possibly, MMP-9 may affect ECM proteolytic

enzymes, allowing the migration of cells into the wound site, which results in the deposition of new ECM and the development of new tissue. However, it is known that the increased presence of TNF- $\alpha$  in diabetes could reduce the MMP-9/TIMP-2 balance production by fibroblasts, contributing to the elevated proteolytic activity impairing wound healing [48].

As expected, and in agreement with the literature [49], type 1 collagen was the most expressed form of collagen in the skin, serving as the framework for connective tissues such as skin, bone and tendons. This result also agrees with the observed increase in the expression of TGF (Figure S3 supplementary data) which has an important role in the pathophysiology of tissue repair by the enhancement of type 1 collagen gene expression [50].

In addition, at day 3, we observed an increased expression of all types of analyzed collagen in control compared to diabetic skin at the same time point and the opposite is verified at day 10 suggesting that diabetes impair collagen gene expression and deposition in the skin [51]. Moreover, the NT-loaded MPC foam stimulated COL1A1, COL1A2 and COL3A1 expression at day 10 in diabetic skin, which is also correlated with higher collagen production observed by the hydroxyproline content and the Masson's Trichrome staining.

656

## 5. Conclusions

The results obtained in this work show that, in control animals, both MPC and NT-loaded MPC foams have great impact on the early phases of the healing process decreasing the inflammatory infiltrate. In diabetic animals, the major healing effects were observed with either NT alone or NT-loaded MPC foams thus confirming the potential healing effect of NT in diabetic wound. These treatments reduced the inflammatory status in the early phase of wound healing and increased migration of fibroblast and collagen expression and deposition for tissue repair. However, a more pronounced scar was observed with the application of MPC. Table 5 summarizes cytokine expression in wounded control and diabetic skin, at day 3 and 10 post-wounding.

These results suggest that *in vivo* NT combined with the MPC foam application in diabetic wound dressings can promote an inflammatory response was able to reduce the inflammatory response, to promote an anti-inflammatory response and to stimulate re-

epithelialization which are important phases of the healing process. Human studies are needed to further investigate the potential application of NT-loaded MPC wound dressings as therapy for diabetic foot ulcers.

674

## 675 **Acknowledgments**

This work was financially supported by COMPETE , FEDER and Fundação para a Ciência e Tecnologia (FCT-MEC) under contract PTDC/SAU-MII/098567/2008, PTDC/SAU FAR/121109/2010 and PEst-C/EQB/UI0102/2011 and PEst-C/SAU/LA0001/2013-2014, in addition to the EFSD/JDRF/Novo Nordisk European Programme in Type 1 Diabetes Research and Sociedade Portuguesa de Diabetologia (SPD).

Liane I. F. Moura, Ana M. A. Dias and Ermelindo Leal acknowledge FCT-MEC for their fellowships SFRH/BD/60837/2009, SFRH/BPD/40409/2007 and SFRH/BPD/46341/2008, respectively.

685

## 686 **Conflict of interest**

The authors declare no competing financial interest.

688

## 689 **Supplementary data**

Supplementary data associated with this article can be found, in the online version, at doi: (to include later).

692

## 693 **References**

694

- 695 [1] Moura LI, Dias AM, Carvalho E, de Sousa HC. Recent advances on the  
696 development of wound dressings for diabetic foot ulcer treatment-A review. *Acta*  
697 *biomaterialia* 2013.
- 698 [2] Tellechea A, Leal E, Veves A, Carvalho E. Inflammatory and angiogenic  
699 abnormalities in diabetic wound healing: role of neuropeptides and therapeutic  
700 perspectives *The Open Circulation and Vascular Journal* 2010;3:43-55.
- 701 [3] Silva L, Carvalho E, Cruz MT. Role of neuropeptides in skin inflammation and its  
702 involvement in diabetic wound healing. *Expert Opin Biol Ther* 2010;10:1427-39.
- 703 [4] Pradhan L, Nabzyk C, Andersen ND, LoGerfo FW, Veves A. Inflammation and  
704 neuropeptides: the connection in diabetic wound healing. *Expert Rev Mol Med*  
705 2009;11:e2.
- 706 [5] Lazarus LH, Brown MR, Perrin MH. Distribution, localization and characteristics of  
707 neurotensin binding sites in the rat brain. *Neuropharmacology* 1977;16:625-9.



- 708 [6] Sundler F, Hakanson R, Hammer RA, Alumets J, Carraway R, Leeman SE, et al.  
709 Immunohistochemical localization of neurotensin in endocrine cells of the gut. *Cell and*  
710 *tissue research* 1977;178:313-21.
- 711 [7] Brain SD. Sensory neuropeptides: their role in inflammation and wound healing.  
712 *Immunopharmacology* 1997;37:133-52.
- 713 [8] Kalafatakis K, Triantafyllou K. Contribution of neurotensin in the immune and  
714 neuroendocrine modulation of normal and abnormal enteric function. *Regulatory*  
715 *peptides* 2011;170:7-17.
- 716 [9] Scott JR, Tamura RN, Muangman P, Isik FF, Xie C, Gibran NS. Topical substance P  
717 increases inflammatory cell density in genetically diabetic murine wounds. *Wound*  
718 *Repair and Regeneration* 2008;16:529-33
- 719 [10] Pradhan L, Cai X, Wu S, Andersen ND, Martin M, Malek J, et al. Gene expression  
720 of pro-inflammatory cytokines and neuropeptides in diabetic wound healing. *J Surg Res*  
721 2011;167:336-42.
- 722 [11] Sweitzer SM, Fann SA, Borg TK, Baynes JW, Yost MJ. What is the future of  
723 diabetic wound care? *The Diabetes Educator* 2006;32:197-210.
- 724 [12] Malafaya PB, Silva GA, Reis RL. Natural-origin polymers as carriers and scaffolds  
725 for biomolecules and cell delivery in tissue engineering applications. *Adv Drug Deliv*  
726 *Rev* 2007;59:207-33.
- 727 [13] Sell SA, Wolfe PS, Garg K, McCool JM, Rodriguez IA, Bowlin GL. The use of  
728 natural polymers in tissue engineering: a focus on electrospun extracellular matrix  
729 analogues. *Polymers for Advanced Technologies* 2010;2:522-53.
- 730 [14] Rinaudo M. Chitin and chitosan: properties and applications. *Progress in Polymer*  
731 *Science* 2006;31:603-32.
- 732 [15] Park CJ, Clark SG, Lichtensteiger CA, Jamison RD, Johnson AJW. Accelerated  
733 wound closure of pressure ulcers in aged mice by chitosan scaffolds with and without  
734 bFGF. *Acta biomaterialia* 2009;5:1926-36
- 735 [16] Huang S, Fu X. Naturally derived materials-based cell and drug delivery systems in  
736 skin regeneration. *Journal of controlled release : official journal of the Controlled*  
737 *Release Society* 2010;142:149-59.
- 738 [17] Dai T, Tanaka M, Huang YY, Hamblin MR. Chitosan preparations for wounds and  
739 burns: antimicrobial and wound-healing effects. *Expert review of anti-infective therapy*  
740 2011;9:857-79.
- 741 [18] Takei T, Nakahara H, Ijima H, Kawakami K. Synthesis of a chitosan derivative  
742 soluble at neutral pH and gellable by freeze-thawing, and its application in wound care.  
743 *Acta biomaterialia* 2012;8:686-93.
- 744 [19] Berscht PC, Nies B, Liebendorfer A, Kreuter J. Incorporation of basic fibroblast  
745 growth factor into methylpyrrolidinone chitosan fleeces and determination of the in  
746 vitro release characteristics. *Biomaterials* 1994;15:593-600.
- 747 [20] Dai YN, Li P, Zhang JP, Wang AQ, Wei Q. A novel pH sensitive N-succinyl  
748 chitosan/alginate hydrogel bead for nifedipine delivery. *Biopharmaceutics & drug*  
749 *disposition* 2008;29:173-84.
- 750 [21] Tan Y, Han F, Ma S, Yu W. Carboxymethyl chitosan prevents formation of broad-  
751 spectrum biofilm. *Carbohydr Polym* 2011;84:1365-70.
- 752 [22] Chen X, Wang Z, Liu W, Park H. The effect of carboxymethyl-chitosan on  
753 proliferation and collagen secretion of normal and keloid skin fibroblasts.  
754 2002;23:4609-14.
- 755 [23] Prabakaran M. Review Paper: Chitosan Derivatives as Promising Materials for  
756 Controlled Drug Delivery. *J Biomater Appl* 2008;23:5-38.

- 757 [24] Muzzarelli RAA, Ilari P, Tomasetti M. Preparation and characteristic properties of  
758 5-methyl pyrrolidinone chitosan. *Carbohydrate Polymers* 1993;20:99-105.
- 759 [25] Santos KSCR, Silva HSRC, Ferreira EI, Bruns RE. 32Factorial design and  
760 response surface analysis optimization of N-carboxybutylchitosan synthesis.  
761 *Carbohydrate Polymers* 2005;59:37-42.
- 762 [26] Dias AMA, Rey-Ricob A, Oliveira RA, Marceneiro S, Alvarez-Lorenzo C,  
763 Concheiro A, et al. Wound dressings loaded with an anti-inflammatory jucá (*Libidibia*  
764 *ferrea*) extract using supercritical carbon dioxide technology. *The Journal of*  
765 *Supercritical Fluids* 2013;74:34-45.
- 766 [27] Brun P, Mastrotto C, Beggiao E, Stefani A, Barzon L, Sturniolo GC, et al.  
767 Neuropeptide neurotensin stimulates intestinal wound healing following chronic  
768 intestinal inflammation. *Am J Physiol Gastrointest Liver Physiol* 2005;288:G621-9.
- 769 [28] da Silva L, Neves BM, Moura L, Cruz MT, Carvalho E. Neurotensin  
770 downregulates the pro-inflammatory properties of skin dendritic cells and increases  
771 epidermal growth factor expression. *Biochim Biophys Acta* 2011;1813:1863-71.
- 772 [29] Obara K, Ishihara M, Fujita M, Kanatani Y, Hattori H, Matsui T, et al.  
773 Acceleration of wound healing in healing-impaired db/db mice with a  
774 photocrosslinkable chitosan hydrogel containing fibroblast growth factor-2. *Wound*  
775 *repair and regeneration* : official publication of the Wound Healing Society [and] the  
776 European Tissue Repair Society 2005;13:390-7.
- 777 [30] Rossi S, Marciello M, Sandri G, Ferrari F, Bonferoni MC, Papetti A, et al. Wound  
778 Dressings Based on Chitosans and Hyaluronic Acid for the Release of Chlorhexidine  
779 Diacetate in Skin Ulcer Therapy. *Pharmaceutical Development and Technology*  
780 2007;12:415-22.
- 781 [31] Huang P, Han B, Liu W, Chang Q, Dong W. Preparation and Biocompatibility of  
782 N-carboxymethyl chitosan. *Journal of Functional Materials* 2009;7:25-33.
- 783 [32] Hwang SM, Chen CY, Chen SS, Chen JC. Chitinous materials inhibit nitric oxide  
784 production by activated RAW 264.7 macrophages. *Biochemical and biophysical*  
785 *research communications* 2000;271:229-33.
- 786 [33] Yang C, Zhou Y, Zhang X, Huang X, Wang M, Han Y, et al. A green fabrication  
787 approach of gelatin/CM-chitosan hybrid hydrogel for wound healing. *Carbohydrate*  
788 *Polymers* 2010;82:1297-305.
- 789 [34] Chen R, Wang G, Chen C, Ho H, Shen M. Development of a new N-O-  
790 (Carboxymethyl)/chitosan /collagen matrixes as a wound dressing. *Biomacromolecules*  
791 2006;7:1058-64.
- 792 [35] Muzzarelli R. Depolymerization of methyl pyrrolidinone chitosan by lysozyme.  
793 *Carbohydrate Polymers* 1992;19:29-34.
- 794 [36] Enoch S, Leaper DJ. Basic Science of wound healing. *Surgery* 2008;26:31-7.
- 795 [37] Davidson JM. Animal models for wound repair. *Archives of dermatological*  
796 *research* 1998;290 Suppl:S1-11.
- 797 [38] Lehr C, Bouwstra JA, Schacht EH, Junginger HE. In vitro evaluation of  
798 mucoadhesive properties of chitosan and some other natural polymers. *International*  
799 *Journal of Pharmaceutics* 1992;78:43-8.
- 800 [39] Ono I, Tateshita T, Inoue M. Effect of a collagen matrix containing basic fibroblast  
801 growth factor on wound contraction. *J Biomed Mater Res (Appl Biomater)*  
802 1999;48:621-30.
- 803 [40] Ishihara M, Ono K, Sato M, Nakanishi K, Saito Y, Yura H, et al. Acceleration of  
804 wound contraction and healing with a photocrosslinkable chitosan hydrogel. *Wound*



- 805 repair and regeneration : official publication of the Wound Healing Society [and] the  
806 European Tissue Repair Society 2001;9:513-21.
- 807 [41] Galkowska H, Wojewodzka U, Olszewski WL. Chemokines, cytokines, and  
808 growth factors in keratinocytes and dermal endothelial cells in the margin of chronic  
809 diabetic foot ulcers. Wound repair and regeneration : official publication of the Wound  
810 Healing Society [and] the European Tissue Repair Society 2006;14:558-65.
- 811 [42] Hansen SL, Myers CA, Charboneau A, Young DM, Boudreau N. HoxD3  
812 accelerates wound healing in diabetic mice. The American journal of pathology  
813 2003;163:2421-31.
- 814 [43] Bashir MM, Sharma MR, Werth VP. TNF-alpha production in the skin. Archives  
815 of dermatological research 2009;301:87-91.
- 816 [44] Lin Z, Kondo T, Ishida Y, Takayasu T, Mukaida N. Essential involvement of IL-6  
817 in the skin wound-healing process as evidenced by delayed wound healing in IL-6  
818 deficient mice. Journal of Leukocyte Biology 2003;73:713-21.
- 819 [45] Gabbiani G. The myofibroblast in wound healing and fibrocontractive diseases.  
820 The Journal of pathology 2003;200:500-3.
- 821 [46] Diegelmann RF, Evans MC. Wound healing: an overview of acute, fibrotic and  
822 delayed healing. Frontiers in bioscience : a journal and virtual library 2004;9:283-9.
- 823 [47] Singer AJ, Clark RA. Cutaneous wound healing. N Engl J Med 1999;341:738-46.
- 824 [48] Blakytyn R, Jude EB. Altered molecular mechanisms of diabetic foot ulcers. Int J  
825 Low Extrem Wounds 2009;8:95-104.
- 826 [49] Crane NJ, Brown TS, Evans KN, Hawksworth JS, Hussey S, Tadaki DK, et al.  
827 Monitoring the healing of combat wounds using Raman spectroscopic mapping. Wound  
828 Repair Regen 2010;18:409-16.
- 829 [50] Verrecchia F, Mauviel A. TGF-beta and TNF-alpha: antagonistic cytokines  
830 controlling type I collagen gene expression. Cellular signalling 2004;16:873-80.
- 831 [51] Black E, Vibe-Petersen J, Jorgensen LN, Madsen SM, Agren MS, Holstein PE, et  
832 al. Decrease of collagen deposition in wound repair in type 1 diabetes independent of  
833 glycemic control. Arch Surg 2003;138:34-40.

# 835 **Figures Captions**

836  
837 Figure 1. A) Chemical synthesis of chitosan derivatives: *N*-carboxymethyl chitosan  
838 (CMC), 5-methyl pyrrolidinone chitosan (MPC) and *N*-succinyl chitosan (SC). B) SEM  
839 micrographs for non-loaded chitosan derivatives CMC, MPC and SC representing the  
840 different structures obtained by freeze-drying. Inner images represent magnifications.

841  
842 Figure 2. Water vapor (A) and water (B) swelling profiles observed for CMC (■), MPC  
843 (▲) and SC (◆) foams. The inserted figure represents a zoom of the water swelling  
844 profiles for the first monitored day. Lines serve only as guides for the eye. Results are  
845 presented as mean  $\pm$  SEM of two independent experiments.

Figure 3. Release kinetic profiles for GSH from CMC (■), MPC (▲) and SC (◆) foams at pH 7 measured for 8 h at 37 °C. Lines serve only as guides for the eye. Results are presented as mean  $\pm$  SEM of two independent experiments.

850

Figure 4. Cell viability of Raw (A) and HaCaT (B) cells in the presence of CMC or MPC foams, during 24, 48 and 72 h. and NO production in Raw cells (C). Results are presented as mean  $\pm$  SEM of three independent experiments.

854

Figure 5. Wound size measurements for MPC, NT and NT-loaded MPC foam treatments in either control (A) or diabetic (B) mice. The wound size was determined at days 0, 1, 3, 5, 8 and 10 post-wounding. Results are presented as mean  $\pm$  SEM of seven to eighteen independent experiments. \* $p < 0.05$  MPC compared to PBS, \*\* $p < 0.01$  MPC compared to PBS, \*\*\*  $p < 0.001$  MPC compared to PBS, #  $p < 0.05$  MPC+NT compared to PBS, ##  $p < 0.01$  MPC+NT compared to PBS, ###  $p < 0.001$  MPC+NT compared to PBS, \$  $p < 0.05$  NT compared to PBS, \$\$  $p < 0.01$  NT compared to PBS; § $p < 0.05$  NT compared to MPC+NT, §§  $p < 0.01$  NT compared to MPC+NT, &&  $p < 0.01$  MPC compared to MPC+NT.

864

Figure 6. The gene expression profile for TNF- $\alpha$ , IL-6, KC, IL-1 $\beta$ , COL1A1, COL1A2 and COL3A1 in skin biopsies before and after treatments, at either day 3 (A, C, E, G, I, K, M) or 10 (B, D, F, H, J, L, N) post wounding. Results are presented as mean  $\pm$  SEM of seven to eighteen independent experiments. &  $p < 0.05$  compared with PBS d3, \* $p < 0.05$  compared with PBS d10, \*\* $p < 0.01$  compared with PBS d10 §  $p < 0.05$  compared with diabetic PBS d3, #  $p < 0.05$  compared with diabetic PBS d10, # # $p < 0.01$  compared with diabetic PBS d10.

872

Figure 7. Protein expression of TNF- $\alpha$  and MMP-9 in unwounded skin (day 0) or after treatments, at either day 3 or 10 post-wounding. Results are presented as mean  $\pm$  SEM of three to five independent experiments. &  $p < 0.05$  compared with PBS d3, \* $p < 0.05$  compared with PBS d10, \*\* $p < 0.01$  compared with PBS d10 §  $p < 0.05$  compared with diabetic PBS d3, #  $p < 0.05$  compared with diabetic PBS d10, # # $p < 0.01$  compared with diabetic PBS d10.

879

880 Figure 8. Hydroxyproline content levels in unwounded skin (d0) or after treatments, at  
881 either day 3 or 10 post-wounding. Results are presented as mean  $\pm$  SEM of four to six  
882 independent experiments. \* $p < 0.05$  compared with PBS d10, §  $p < 0.05$  compared with  
883 diabetic PBS d3, #  $p < 0.01$  compared with diabetic PBS d10.

884

885 Figure 9. Histopathological analysis of Hematoxylin and Eosin (H&E) (Figure 9A)  
886 and Masson's Trichrome (Figure 9B) staining for control and diabetic mouse skin,  
887 untreated or treated with MPC, NT and NT-loaded MPC foams (magnification 100 $\times$ ).  
888 Representative images of three skin stainings analyzed. a) Different repair process: in  
889 diabetic wounds, the granulation tissue is retained in dermis with overgoing fibroblast  
890 proliferation, at day 3 post-wounding (H&E; magnification 200 $\times$ ); b) Infiltrated PMN  
891 and lymphocytes in the granulation tissue in control mice, at day 3 post-wounding  
892 (H&E; magnification: 200 $\times$ ); c) Persistent inflammatory cells (neutrophils and lympho-  
893 plasmocytic cells) in PBS-treated diabetic mice, at day 10 post-wounding (H&E;  
894 magnification: 200 $\times$ ); d) Less inflammatory cells in granulation tissue when compared  
895 with c) in MPC-treated wounds, at day 10 post-wounding (H&E; magnification: 200 $\times$ );  
896 e) Less deposition of collagen in PBS-treated diabetic mice, at day 10 post-wounding  
897 (Masson's Trichrome; magnification: 200 $\times$ ); f) The granulation tissue is formed mainly  
898 by thin collagen fibers parallel to the epidermis (Masson's Trichrome).

899

900 Supplementary data S1:  $^1\text{H}$ -RMN spectra of chitosan, CMC, MPC and SC foams.

901

902 Supplementary data S2: Release kinetic profiles for GSH from CMC (■), MPC (▲) and  
903 SC (◆) foams at pH 6 (A) and 8 (B) measured for 8 h at 37 °C. Lines serve only as  
904 guides for the eye. Results are presented as mean  $\pm$  SEM of two independent  
905 experiments.

906

907 Supplementary data S3: The gene expression profile for MMP-9, EGF, VEGF, PDGF,  
908 TGF $\beta$ 1 and TGF $\beta$ 3, in skin biopsies before and after treatments, at either day 3 (A, C,  
909 E, G, I, K) or 10 (B, D, F, H, J, L) post wounding. Results are presented as mean  $\pm$   
910 SEM of seven to eighteen independent experiments. &  $p < 0.05$  compared with PBS d3,  
911 \* $p < 0.05$  compared with PBS d10, \*\* $p < 0.01$  compared with PBS d10 §  $p < 0.05$

912 compared with diabetic PBS d3, #  $p < 0.05$  compared with diabetic PBS d10, #  $p <$   
913 0.01 compared with diabetic PBS d10.  
914

ACCEPTED MANUSCRIPT

## List of tables

**Table 1:** Histological analysis of unwounded skin and NT, MPC and NT loaded MPC foams treated wounds at day 3, by H&E staining. - absence or no alterations, + presence <10%, ++ presence 10%,-50%, n.a, not applicable

	Skin control (d0)		Day 3							
			PBS		MPC		NT		MPC+NT	
	Control	Diabetic	Control	Diabetic	Control	Diabetic	Control	Diabetic	Control	Diabetic
New epidermis thickness										
- Stratus lucidum	-	+	-	+	+	++	-	+	+	++
- Epithelial layers	-	+	-	+	+	++	-	+	+	++
- Basal layer	-	+	-	+	+	++	-	+	+	++
Wound area (mm <sup>2</sup> )	26.48 ±4.22	27.71±5.41	30.30±0.17	29.02±0.32	18.68±0.12	22.64±0.22	24.53±0.31	20.95±0.34	17.80±0.18	16.68±0.17
Re-epithelization										
- From bottom	na	na	+	-	+	-	+	-	+	-
- Top cover	na	na	-	+	-	+	-	+	-	+

**Table 2:** Histological analysis of NT, MPC and NT loaded MPC foams treated wounds at day 10, by H&E staining. - absence or no alterations, + presence <10%, ++ presence 10%,-50%, +++ presence >50%

	Day 10							
	PBS		MPC		NT		MPC+NT	
	Control	Diabetic	Control	Diabetic	Control	Diabetic	Control	Diabetic
New epidermis thickness								
- Stratus lucidum	++	+++	+	++	++	+++	+	++
- Epithelial layers	++	+++	+	++	++	+++	+	++
- Basal layer	++	+++	+	++	++	+++	+	++
Wound area (mm <sup>2</sup> )	9.02±0.15	13.39±0.31	4.22±0.09	12.11±0.20	7.05±0.30	9.12±0.30	5.88±0.12	9.77±0.29
Re-epithelization								
- From bottom	+	-	+	-	+	-	+	-
- Top cover	-	+	-	+	-	+	-	+

**Table 3:** Inflammatory and granulation tissue histological analysis of NT, MPC and NT loaded MPC foams treated wounds at day 3, by H&E and Masson's Trichrome staining. - absence or no alterations, + presence <10%, ++ presence 10%,-50%, +++ presence >50%; < not relevant, > predominant

	Day 3							
	PBS		MPC		NT		MPC+NT	
	Control	Diabetic	Control	Diabetic	Control	Diabetic	Control	Diabetic
Inflammation Status								
- PMN	++	+++	++	+	++	+	++	+
- Lymphocytes	+	++	+	-	+	-	+	-
- Plasma cells	-	-	-	-	-	-	-	-
- Fibrin	<	>	>	<	>	<	>	<
Repair								
- Fibroblasts	<	>	<	>	<	>	<	>
Collagen matrix								
- Loose	-	-	-	+	+	+	+	-
- Scar	-	-	-	+	-	+	+	++

**Table 4:** Inflammatory and granulation tissue histological analysis of NT, MPC and NT loaded MPC foams treated wounds at day 10, by H&E and Masson's Trichrome staining. - absence or no alterations, + presence <10%, ++ presence 10%,-50%, +++ presence >50%;

	Day 10							
	PBS		MPC		NT		MPC+NT	
	Control	Diabetic	Control	Diabetic	Control	Diabetic	Control	Diabetic
Inflammation Status								
- PMN	-	++	-	+	-	+	-	+
- Lymphocytes	+	+++	+	++	+	++	+	++
- Plasma cells	+	+++	+	++	+	++	+	++
- Fibrin	-	-	-	-	-	-	-	-
Repair								
- Fibroblasts	++	+	+	++	+	+	+	+++
Collagen matrix								
- Loose	-	-	-	-	-	-	-	-
- Scar	++	+	+	++	+	+	+	+++

**Table 5:** Summary of cytokine and protein expression in wounded control and diabetic skin, at day 3 and 10 post-wounding.

Day	Cytokine/Growth factor	Control mice	Diabetic mice	Cell type that produce this protein
3	TNF- $\alpha$	↓ MPC, NT, MPC+NT	↑ NT, MPC+NT	Macrophages, fibroblasts
	IL-6	↓ MPC; ↑ MPC+NT	↓ MPC, NT, MPC+NT	Macrophages, fibroblasts, Keratinocytes, endothelial cells
	KC	↑ MPC+NT	↓ MPC, NT, MPC+NT	Macrophages, fibroblasts
	IL-1 $\beta$	↓ MPC, NT, MPC+NT	= MPC, NT, MPC+NT	Macrophages, epithelial cells
	COL1A1	=	↑ NT	Fibroblasts
	COL1A2	=	↑ NT	Fibroblasts
	COL3A1	↑ MPC+NT	↑ NT	Fibroblasts
10	TNF- $\alpha$	↑ NT, MPC+NT	↓ NT, MPC+NT	Macrophages, fibroblasts
	IL-6	=	↓ MPC, NT, MPC+NT	Macrophages, fibroblasts, keratinocytes, endothelial cells
	KC	=	↓ MPC, NT, MPC+NT	Macrophages, fibroblasts
	IL-1 $\beta$			Macrophages, epithelial cells
	COL1A1	↑NT,MPC+NT	↑MPC+NT	Fibroblasts
	COL1A2	↑NT,MPC+NT	↑MPC+NT	Fibroblasts
	COL3A1	↑NT	↑MPC+NT	Fibroblasts

